Journal of Alloys and Compounds 630 (2015) 292–298

Contents lists available at ScienceDirect

Journal of Alloys and Compounds

journal homepage: www.elsevier.com/locate/jalcom

Cu–Li_2MnSiO_4-polyaniline composite hybrids as high performance cathode for lithium batteries

Sol-Nip Lee [a], Seulgi Baek [a], Samuthirapandian Amaresh [a], Vanchiappan Aravindan [a,b], Kyung Yoon Chung [c], Byung Won Cho [c], Won-Sub Yoon [d,*], Yun-Sung Lee [a,*]

[a] Faculty of Applied Chemical Engineering, Chonnam National University, Gwang-ju 500-757, Republic of Korea
[b] Energy Research Institute @ NTU (ERI@N), Nanyang Technological University, Research Techno Plaza, 50 Nanyang Drive, Singapore 637553, Singapore
[c] Center for Energy Convergence, Korea Institute of Science and Technology, Seoul 136-791, Republic of Korea
[d] Department of Energy Science, Sungkyunkwan University, Suwon 440-746, Republic of Korea

ARTICLE INFO

Article history:
Received 11 November 2014
Received in revised form 30 December 2014
Accepted 11 January 2015
Available online 17 January 2015

Keywords:
Lithium-ion battery
Cathode
Orthosilicate
Beyond one electron reaction

ABSTRACT

We reported the dramatic improvement in electrochemical properties of high capacity orthosilicate, Li_2MnSiO_4 by conventional sol–gel route. Simple inclusion of metallic Cu and subsequent hybridization with polyaniline (PANI) nanofibers certainly promotes superior electrochemical activity in terms of high reversibility i.e. beyond one electron reaction and cycling stability. First, the Li_2MnSiO_4 nanoparticles are prepared by adipic acid assisted sol–gel technique at 700 °C under Ar flow by fine tuning the sintering duration. Then, optimization of adipic acid and Cu concentrations are performed based on the mentioned sintering conditions to yield high performance cathode active material. The Cu–Li_2MnSiO_4-PANI hybrid exhibits the reversible insertion of ~1.15 and 0.73 mol of Li for first and 50th cycles, respectively. This corresponds to the ~63% of retention.

1. Introduction

Development of high energy density Li-ion power packs is warranted to power the zero emission transportation applications like hybrid electric vehicles and electric vehicles [1,2]. However, the construction of such Li-ion batteries are completely depends on the utilization of high capacity cathodes without compromising the cost-effectiveness, cell-safety and eco-friendliness [3]. In this regard, polyanion framework materials are found attractive and fulfilling the mentioned requirements. Among the polyanions investigated, olivine phase $LiFePO_4$ is one of the perfect examples for the said frameworks [3–8]. However, the lower working potential (~3.4 V *vs.* Li) and capacity (~170 mA h g^{-1}) is insufficient for the afore said applications [9]. Rest of the olivine phase materials $LiMnPO_4$ (~4.1 V *vs.* Li) is experiencing slower Li-diffusion kinetics associated with inferior electrical conductivity, $LiCoPO_4$ (~4.8 V *vs.* Li) suffers $(PO_4)^{3-}$ anion dissolution issue in conventional carbonate based solutions and $LiNiPO_4$ (~5.2 V *vs.* Li) is electrochemically inactive [4]. Apart from the mentioned issues, the theoretical capacity is limited between 160–170 mA h g^{-1} only, though exhibits higher redox potential. Similar to olivine phosphates, orthosilicates composed of general formula Li_2MSiO_4 (M = Fe, Mn, Co) is attracted the researchers owing to the salient features like beyond one electron reaction is possible i.e. exhibits the high theoretical capacity of >330 mA h g^{-1}, high thermal stability in de-lithiated state due to the presence of strong co-valent bond between Si–O, inexpensive and eco-friendliness. Indeed such polyanion framework having the lack of conductivity issues similar to olivine framework materials [10–19]. Therefore, conductive coating or composite with conducting substance is required to overcome the inherent conductivity issues.

In the case of orthosilicate family, Li_2MnSiO_4 is much favourable electrochemical characteristics owing to its high redox potential and possible utilization of Mn^{2+}/Mn^{3+} and Mn^{3+}/Mn^{4+} (~4.1 V *vs.* Li)compared to its counterpart Li_2FeSiO_4 (~2.76 V *vs.* Li). Unfortunately, amorphousization upon cycling and Mn dissolution are the main issues for such Li_2MnSiO_4 cathodes, apart from the intrinsic electrical conductivity (~$10^{-14\sim16}$ S cm^{-1}). However, the Li_2CoSiO_4 (~4.2 V *vs.* Li) is not electrochemically much active compared to Mn and Fe based silicates. Recently, we extensively investigated the electrochemical properties of Li_2MnSiO_4 prepared by various synthetic procedures like solid-state, sol–gel and hydrothermal routes [15–19]. Inclusion of higher amount of carbon loading is one of the efficient ways to suppress the amorphousization upon cycling, but such loading certainly dilutes the volumetric capacity of the system [16]. In this line, we made an attempt to

* Corresponding authors. Tel.: +82 62 530 1904; fax: +82 62 530 1849.
E-mail addresses: wsyoon@skku.edu (W.-S. Yoon), leeys@chonnam.ac.kr (Y.-S. Lee).

http://dx.doi.org/10.1016/j.jallcom.2015.01.047
0925-8388/

employ Cu-inclusion in the into Li_2MnSiO_4 to improve the electrical conductivity along with *in-situ* derived carbon. Since, Cu is an efficient element for either doping or simple mixing without much altering the conducting profiles of the polyanion framework materials, preferably $LiFePO_4$. In addition, polyaniline (PANI)-Cu–Li_2MnSiO_4 composite hybrids also prepared to improve the electrochemical performance. Since improving the electrochemical properties by making composite with conducting polymers like PANI and polypyrrole are one of the remarkable approaches to improve the rate capability and stability of the electrodes, especially cathodes which have been clearly evidenced by us for layered type $Li(MnNiFe)_{1/3}O_2$ material [20,21]. Extensive structural and electrochemical properties are carried out for the optimization and described in detail.

2. Experimental section

Conventional sol–gel route was employed for the preparation of Li_2MnSiO_4. In a typical synthesis procedure, stoichiometric amounts of amounts of starting materials $LiCH_3COO{\cdot}2H_2O$ (Junsei, Japan), $Mn(CH_3COO)_2{\cdot}4H_2O$ (Sigma-Adrich, USA) and $Si(CH_3COO)_4$ (Alfa-Aesar, USA were dissolved separately and mixed together. Ethylene glycol and adipic acids (0.1 M with respect to the total metal ions present in the compound) were also added to the above solution as chelating agents to control the particle size. The sol was dried at 120 °C and subsequently heat treated at 700 °C under Ar flow at various sintering durations (5, 7 and 9 h). For the case of Cu-doping, an appropriate amount of $Cu(CH_3COO)_2$ was incorporated to the above solution and repeating the same synthesis protocol. PANI-Cu–Li_2MnSiO_4 composite hybrids preparation, first the PANI was synthesized by chemical polymerization by dissolving 1 mmol. and 0.2 mol. of aniline and ammonium persulphate separately in 5 ml of 1 M HCl. Highly viscous black coloured precipitate containing PANI was obtained withing 10 min of reaction. Then, appropriate amount of Cu–Li_2MnSiO_4 was added to the above solution and stirred vigorously for 10 min and sonicated them for 3 min. Then the resultant composite was washed several times with de-ionized water and subsequently dried at 60 °C for overnight prior to the powder and electrochemical characterizations.

Powder X-ray diffraction (XRD) measurements were performed using D/MAX Ultiam III, Rigaku Co., Japan equipped with Cu Kα radiation. Morphological features were studies were conducted using field emission scanning electron microscope (FE-SEM, S-4700, Hitachi Co., Japan) with energy dispersive X-ray diffraction attachment (EDX, EX-200, Horiba Co., Japan). The composite electrodes were formulated with accurately weighed 10 mg of active material, 2 mg of Ketjen black (conductive additive) and 1 mg of teflonized acetylene black (TAB-2, binder) using ethanol. Then, the formulated film were pressed over the 200 mm^2 stainless steel mesh (Specac hydraulic press by applying 10 tons) and vacuum dried at 160 °C for 4 h. The half-cells fabricated with metallic lithium which was separated by polypropylene film and filled with 1 M $LiPF_6$ ethylene carbonate (EC)/di-methyl carbonate (DMC) (1:1 by vol., Soulbrain Co., Korea). Galvanostatic cycling profiles were conducted between 1.5 and 4.8 V *vs.* Li at 20 mA g^{-1} in ambient temperature conditions.

3. Results and discussion

Sol–gel route is one of the convenient techniques to prepare nanostructured silicate particles with controlled morphology with high yield. Apart from the synthesis procedure, an appropriate optimization is necessary to obtain high performance cathode active material. Sintering duration is also equally important as that of synthesis temperature. Based on the thermo-gravimetric analysis and previous experience on the synthesis of Li_2MnSiO_4 nanostructures, we have fixed the 700 °C is the optimum temperature to yield the desired phase [15]. At 700 °C, the sintering duration is varied for 5, 7 and 9 h to fine tune synthesis conditions. Fig. 1 represents the XRD pattern of Li_2MnSiO_4 sintered at various sintering duration at 700 °C under Ar flow. Apparent to note that in all the conditions, the desired Li_2MnSiO_4 phase is noted except the trace amount of unavoidable impurity phases like Li_2SiO_3 and MnO [15]. Because of the presence of impurity traces, it is bit difficult to find out the optimum condition to yield high performance cathode. In this line, all the materials prepared at 700 °C are subjected for electrochemical studies to elucidate the high performing cathode. Galvanostatic cycling profiles of above materials are tested between 1.5 and 4.8 V

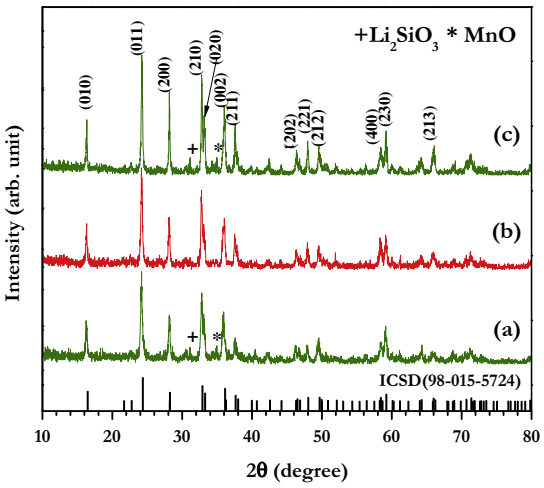

Fig. 1. XRD patterns of Li_2MnSiO_4 materials calcined at different durations. (a) 5 h, (b) 7 h and (c) 9 h.

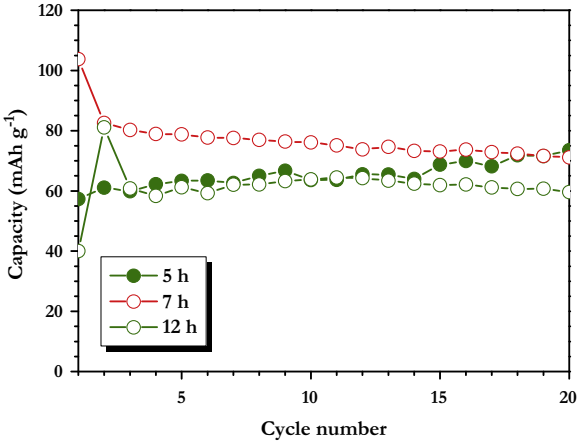

Fig. 2. Galvanostatic cycling profiles of the Li_2MnSiO_4 materials calcined at different durations in half-cell configurations between 1.5 and 4.8 V *vs.* Li at current density of 20 mA g^{-1}.

vs. Li at current density of 20 mA g^{-1} and given in Fig. 2. Unfortunately the extraction of one mole of Li is not possible for the all the three conditions. This clearly shows the inferior electrical conductivity of the prepared Li_2MnSiO_4 phase. Therefore, either carbon coating or making composites with conducting materials are necessary to improve the electrochemical activity. By the way, among the worst performance observed for the silicates prepared at 700 °C, the Li_2MnSiO_4 phase sintered for 7 h is found better in terms of reversibility and stability.

Carbon coating was conducted for the Li_2MnSiO_4 prepared at 700 °C for 7 h by varying the adipic acid concentration. Here, the adipic acid concentration was based on the total amount of metal ion present in the Li_2MnSiO_4 [22]. Fig. 3 depicts the XRD pattern of Li_2MnSiO_4 powders synthesized at 700 °C for 7 h with various adipic acid concentrations (0.1, 0.15, 0.2 and 0.25 M). From the XRD reflections, it is evident that the formation of orthorhombic structure with the expected impurity traces like Li_2SiO_3 and MnO. Apparent the intensity of the impurity traces are found minimum for the case of 0.15 M adipic acid treated compound. Therefore, a good electrochemical profile is anticipated for the mentioned phase. At higher adipic acid concentrations, the dilution of active material takes place owing to the higher amount of pyrolyzed carbon and lower concentration is not sufficient to cover-up the

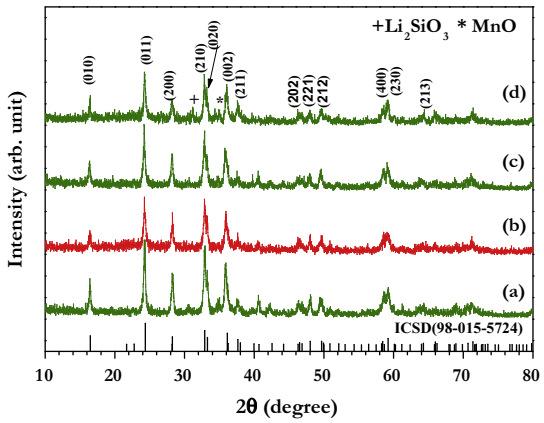

Fig. 3. XRD patterns of Li_2MnSiO_4 materials using adipic acid as chelating agent along with ethylene glycol. The molar ratio of adipic acid to total metal ions with ethylene glycol is (a) 0.1, (b) 0.15, (c) 0.2, and (d) 0.25 mol.

particulates. As a result, slightly increased amount of secondary phases is appeared with varying in adipic acid concentration (except 0.15 M), since in both cases the desired phase is much exposed. However, before conducting electrochemical studies, it is worth to investigate the presence of carbon coating over the Li_2MnSiO_4 particulates. Thus, high resolution TEM (HR-TEM) investigations are performed along with the morphological studies and presented in Fig. 4. From the SEM pictures, at lower concentrations of adipic acid (0.1 M) results the agglomeration of the particles. When the concentration is increased, a highly dispersed particulate morphology is noted with particulate size of ~30–60 nm. Only selected sample (ex. 0.15 M adipic acid) was subjected to HR–TEM studies to ensure the presence of carbon layer. The HR–TEM picture clearly indicates the presence of carbon coating over the Li_2MnSiO_4 particulates with thickness of ~3–4 nm.

Fig. 5 represents the galvanostatic charge–discharge studies of Li_2MnSiO_4 prepared at various concentration of adipic acid between 1.5 and 4.8 V *vs.* Li at current density of 20 mA g^{-1}.

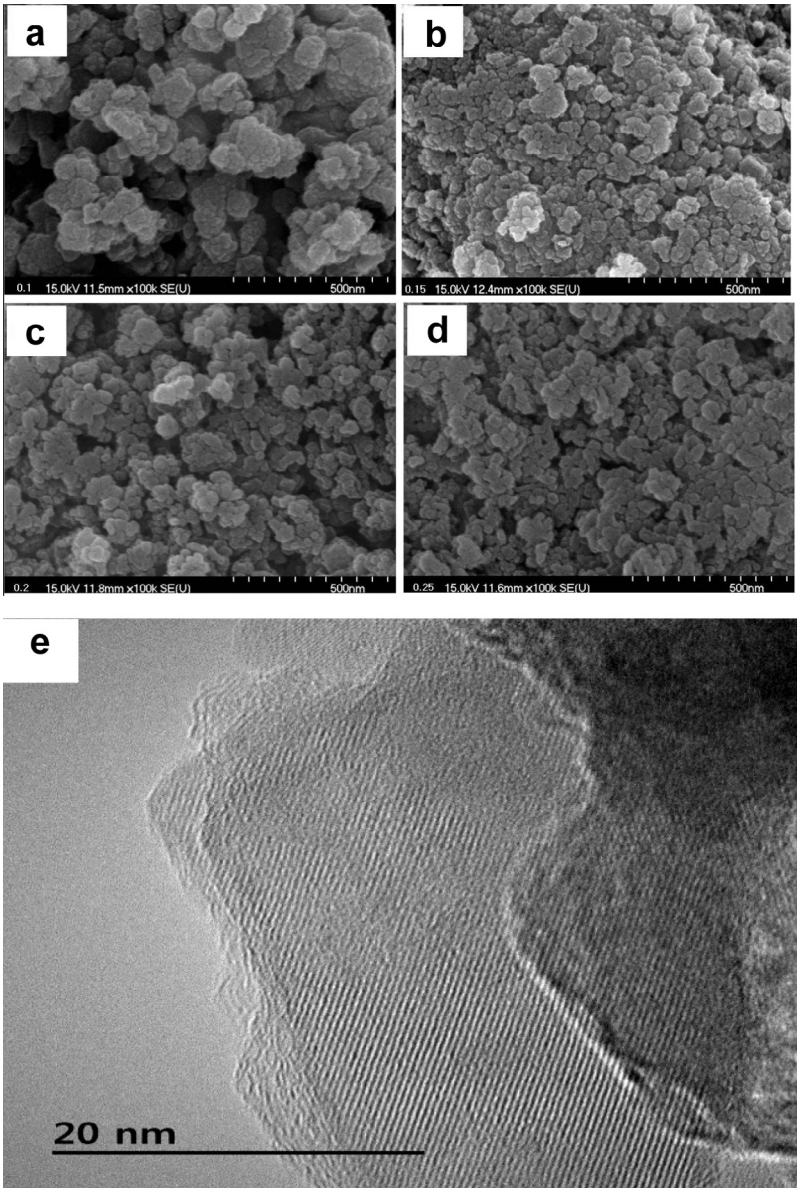

Fig. 4. SEM analysis of Li_2MnSiO_4 materials prepared using adipic acid along with Ethylene glycol as carbon source. The molar ratio of adipic acid to total metal ions with ethylene glycol is (a) 0.1, (b) 0.15, (c) 0.2, and (d) 0.25 mol, (e) HR–TEM image of carbon coated Li_2MnSiO_4 material using as carbon source (0.15 mol).

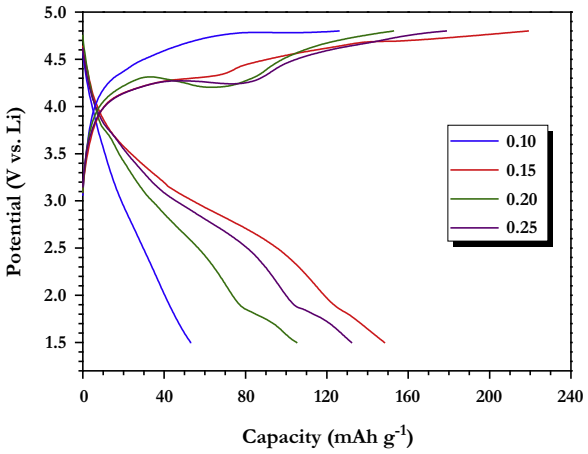

Fig. 5. Initial charge–discharge curves of Li_2MnSiO_4 materials prepared with different molar ratio of adipic acid in half-cell configurations between 1.5 and 4.8 V *vs.* Li at current density of 20 mA g^{-1}.

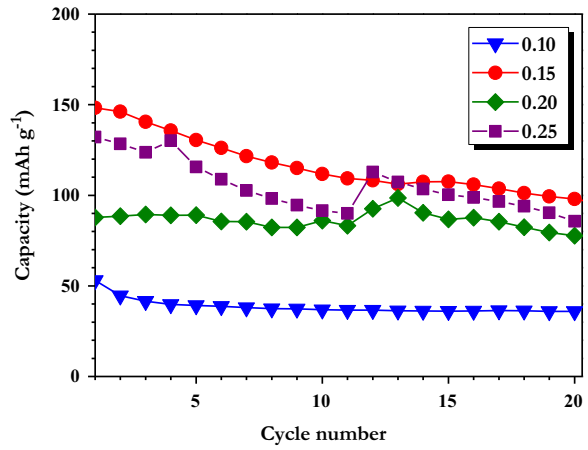

Fig. 6. Cycle performance of Li_2MnSiO_4 materials prepared with different molar ratio of adipic acid.

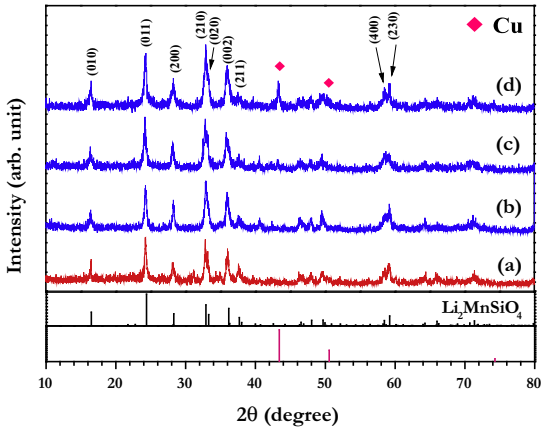

Fig. 7. XRD patterns of Cu-added Li_2MnSiO_4 materials obtained by sol–gel method. (a) Cu = 0, (b) Cu = 0.01, (c) Cu = 0.05, and (d) Cu = 0.1.

Monotonous curve is note during discharge process, which indicates the single phase reaction mechanism of Li_2MnSiO_4 (Fig. 5). There is no linear relationship between capacity profiles and adipic acid concentration observed. Li_2MnSiO_4 prepared with 0.15 M adipic acid delivered the maximum reversible capacity of ~148 mA h g^{-1} which corresponds to the reversible insertion of ~0.9 mol Li per formula unit. Increase in adipic acid concentration results the dilution of active material i.e. *in-situ* derived carbon dilutes the active particle distribution. As a consequence, a decrease in capacity profiles is noted. The observed reversible capacity is almost twice that of the performance in the sintering duration optimization. However, the capacity fading remains an issue and retains only ~66% of initial reversible capacity after 20 cycles (Fig. 6). The cycling profiles are too far behind the application point of view. Moreover, the observed reversible capacity is also in line with other conventional cathodes like $LiFePO_4$, $Li(MnCoNi)_{1/3}O_2$ etc. [23]. Therefore, desperately further improvements are required to make orthorhombic Li_2MnSiO_4 as attractive cathode active material. In this line, we made an attempt to incorporate the metallic Cu as an additive to study the influence in both reversible capacity and stability point of view.

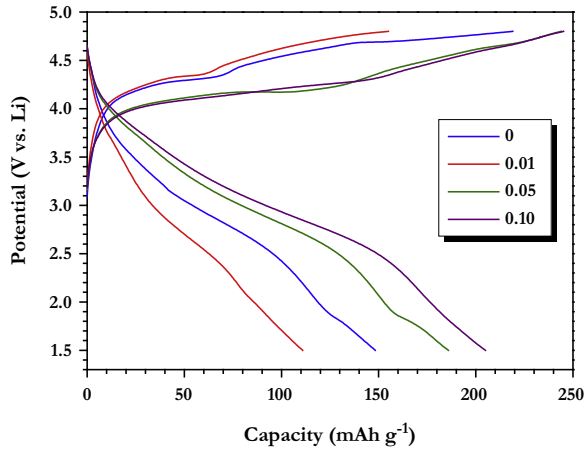

Fig. 8. Typical charge–discharge curves of Cu-added Li_2MnSiO_4 materials with various mol concentrations of Cu.

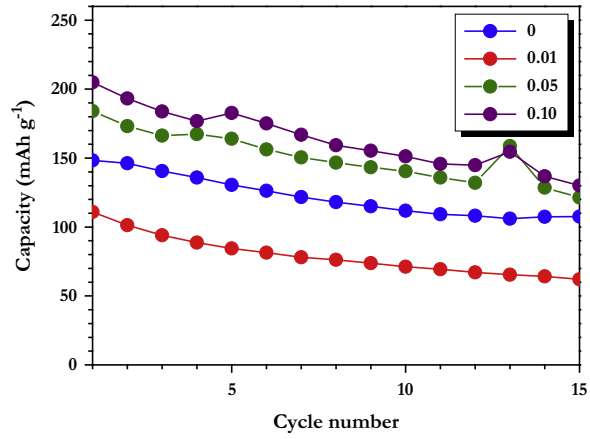

Fig. 9. Cycling performance of Cu-added Li_2MnSiO_4 materials with various concentrations of Cu.

Fig. 7 shows the XRD pattern of Cu-incorporated Li_2MnSiO_4 prepared by 0.15 M adipic acid at 700 °C for 7 h under Ar flow with various Cu concentrations (0.01, 0.05 and 0.1 M). Since, we take the stoichiometric concentrations of the precursors for the preparation of Li_2MnSiO_4, so there is no possibility of Cu-doping, although using the Cu-acetate. In addition, the ethylene glycol is a well known mild reducing agent to form the metallic Cu along with the Li_2MnSiO_4 particulates [24]. The presence of metallic Cu

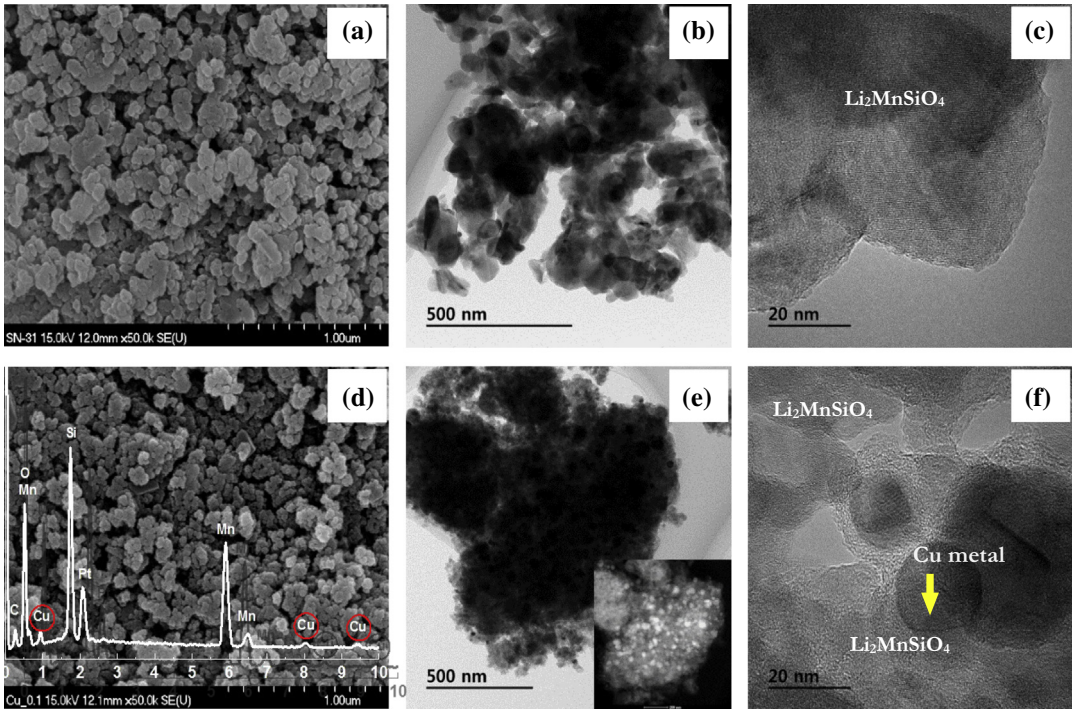

Fig. 10. SEM and TEM images of (a∼c) Li_2MnSiO_4 and (d∼f) Cu-added Li_2MnSiO_4 (Cu = 0.1) cathode materials.

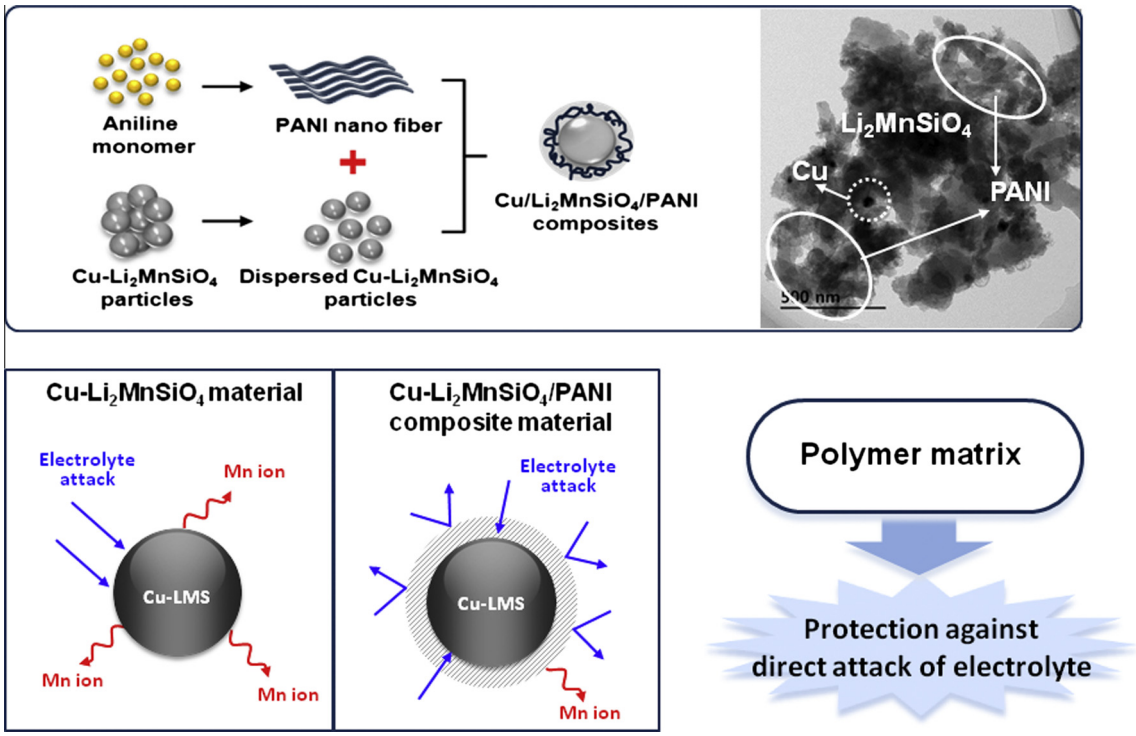

Scheme 1. Schematic illustrations of the synthesis of Cu–Li_2MnSiO_4-PANI composite electrode.

is clearly evident from the XRD reflections, especially at higher concentration (0.1 M). In the lower concentrations, the amount of Cu present in the cathode is either too low or not in the detectable limitations of the X-ray diffractometer. On the other hand, the presence of Cu particles did not affect the formation of the orthorhombic phase. The electrochemical profiles of the Cu-incorporated Li_2MnSiO_4 electrodes are evaluated between 1.5 and 4.8 V *vs.* Li at current density of 20 mA g^{-1} and Fig. 8. Small amount of Cu incorporation (0.01 M) offers lower capacity than bare one. However, further increase in Cu concentration results the increase in the reversibility of Li, for instance the reversible capacity of ∼186 (1.09 mol Li) and ∼205 mA h g^{-1} (1.23 mol Li) is observed for 0.05 and 0.1 M of Cu incorporation, respectively. The inclusion of Cu into the silicates is twofold, (a) increase the Li-ion diffusion

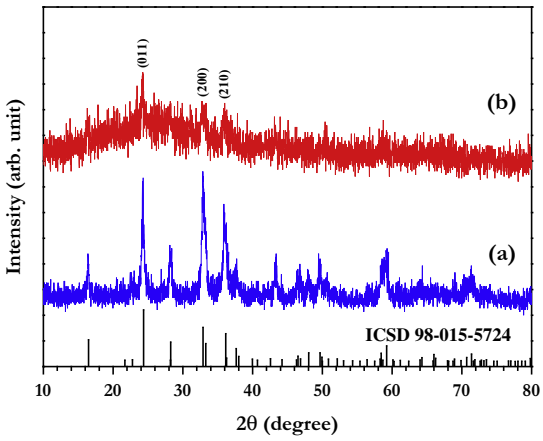

Fig. 11. XRD patterns of (a) Cu-added Li_2MnSiO_4 and (b) Cu-added Li_2MnSiO_4/PANI composite materials.

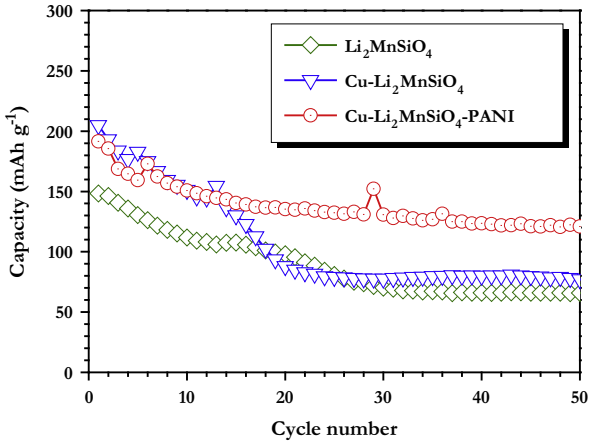

Fig. 12. Cycling performances of Li_2MnSiO_4, Cu–Li_2MnSiO_4 and Cu–Li_2MnSiO_4-PANI composite materials in half-cell assembly between 1.5 and 4.8 V *vs.* Li at current density of 20 mA g^{-1}.

kinetics (Fig. S1) and (b) offers lower charge-transfer resistance (Fig. S2). Although several attempts like carbon coating and Cu-incorporation is carried out, but the capacity fading has not been completely circumvented for example the half-ells retained the reversible capacity of only ~125–130 mA h g^{-1} after 15 cycles (Fig. 9). Before conducting the further studies to improve capacity retention properties, morphological features of the Cu-incorporated Li_2MnSiO_4 nanostructures are worth to investigate.

Morphological features of the Cu-incorporated Li_2MnSiO_4 nanostructures were evaluated by means of FE-SEM and TEM along with EDX measurements and given in Fig. 10. There is no obvious difference between the particulate morphologies is noted for both cases (Fig. 10a and d). The formation of metallic particles are evidenced in XRD measurements while using high concentration of Cu (0.1 M). Thus, Cu incorporated Li_2MnSiO_4 is subjected to TEM analysis (0.1 M). The presence of Cu nanoparticle is clearly evident from the HR–TEM pictures and also well supported from the EDX measurements as well. This clearly suggests the presence of ethylene glycol certainly acts as the reducing agents and no Cu-doping takes place.

The best performing Cu-incorporated Li_2MnSiO_4 (0.1 M) composite was prepared with PANI by chemical polymerization process. The schematic representation of the possible synthesis procedure is illustrated Scheme 1. The usage of PANI is in two for the battery applications especially Mn based materials. Generally, Mn dissolution is one of the important issues for the conventional carbonate based solutions, irrespective of the crystal structure. The PANI wiring over carbon coated Li_2MnSiO_4 certainly avoid the direct contact with the electrolyte counterpart. Therefore, less Mn dissolution and amorphousization is anticipated for the PANI wired Cu-incorporated Li_2MnSiO_4. The XRD pattern clearly revealed the presence of PANI and its influence in the structural prospects (Fig. 11). The XRD pattern clearly revealed the formation of composite with Cu-incorporated Li_2MnSiO_4. However, the prominent reflections of Li_2MnSiO_4 in the PANI wired Cu-incorporated Li_2MnSiO_4 composites are highly disturbed because of the amorphous nature of the PANI. Nevertheless, there is no deviation from the peak positions of Li_2MnSiO_4 are noted, which confirms that PANI does not influence the structural properties of the native phase rather than composite formation.

The electrochemical profiles of PANI wired Cu-incorporated carbon coated Li_2MnSiO_4 (Cu–Li_2MnSiO_4-PANI) were evaluated between 1.5 and 4.8 V *vs.* Li at current density of 20 mA g^{-1}. For comparison purpose, cycling profiles of carbon-coated Li_2MnSiO_4 and Cu-incorporated Li_2MnSiO_4 are also given in Fig. 12. Although, slightly lower capacity (~192 mA h g^{-1}) is noted for Cu–Li_2MnSiO_4-PANI at first cycle compared to Cu–Li_2MnSiO_4 (~204 mA h g^{-1}), but delivered a good capacity retention characteristics. As expected, the C–Li_2MnSiO_4 renders an inferior electrochemical activity compared to the Cu–Li_2MnSiO_4 and Cu–Li_2MnSiO_4-PANI composite hybrids. The capacity retention of ~48, ~34 and ~63% is noted after 50 cycles for C–Li_2MnSiO_4, Cu–Li_2MnSiO_4 and Cu–Li_2MnSiO_4-PANI, respectively. The good capacity retention properties with beyond one electron reaction is certainly achieved from the combined beneficial effects of carbon coating, Cu incorporation and making composite with highly conducting PANI fibers. This certainly improves the volumetric capacity compared to our previous work on the high loading of ~50% carbon to attain the single electron reaction. Further studies are in progress to improve the cycleability of the attracting high capacity cathode active material Li_2MnSiO_4 without compromising the beyond one electron reaction.

4. Conclusion

We successfully demonstrated the substantial improvement in the electrochemical properties of Li_2MnSiO_4 cathodes and realized the beyond one electron reaction. Such improvement could be possible by optimizing the sintering duration, adipic acid concentration (i.e. carbon concentration) and inclusion of Cu particulates in sol–gel technique. The hybridization with PANI nanofibers were cannot be ruled out for the enhancement. The Cu–Li_2MnSiO_4-PANI hybrids delivered the reversible capacity of ~192 mA h g^{-1} and retained ~63% of initial reversible capacity after 50 cycles. This encouraging result certainly provides the new avenues for the development of high performance cathode materials for Li-ion battery applications.

Acknowledgments

This work was supported by the International Cooperation of the Korea Institute of Energy Technology Evaluation and Planning (KETEP) Grant funded by the Korea government Ministry of Knowledge Economy (No. 20128510010050).

Appendix A. Supplementary material

Supplementary data associated with this article can be found, in the online version, at http://dx.doi.org/10.1016/j.jallcom.2015.01.047.

References

[1] V. Aravindan, J. Gnanaraj, Y.-S. Lee, S. Madhavi, Chem. Rev. 114 (2014) 11619–11635.
[2] V. Aravindan, J. Sundaramurthy, P. Suresh Kumar, Y.-S. Lee, S. Ramakrishna, S. Madhavi, Chem. Commun. (2015) 10.1039/C4CC07824A.
[3] V. Aravindan, J. Gnanaraj, Y.S. Lee, S. Madhavi, J. Mater. Chem. A 1 (2013) 3518–3539.
[4] C. Masquelier, L. Croguennec, Chem. Rev. 113 (2013) 6552–6591.
[5] Z. Gong, Y. Yang, Energy Environ. Sci. 4 (2011) 3223–3242.
[6] A.K. Padhi, K.S. Nanjundaswamy, J.B. Goodenough, J. Electrochem. Soc. 144 (1997) 1188–1194.
[7] V. Aravindan, K. Karthikeyan, S. Amaresh, Y.S. Lee, Bull. Korean Chem. Soc. 31 (2010) 1506–1508.
[8] V. Aravindan, M. Umadevi, Ionics 18 (2012) 27–30.
[9] A. Manthiram, Electrochem. Soc. Interface 18 (2009) 44–47.
[10] R.J. Gummow, Y. He, J. Power Sources 253 (2014) 315–331.
[11] R. Dominko, M. Bele, M. Gaberšček, A. Meden, M. Remškar, J. Jamnik, Electrochem. Commun. 8 (2006) 217–222.
[12] M.S. Islam, R. Dominko, C. Masquelier, C. Sirisopanaporn, A.R. Armstrong, P.G. Bruce, J. Mater. Chem. 21 (2011) 9811–9818.
[13] R. Dominko, J. Power Sources 184 (2008) 462–468.
[14] K. Karthikeyan, V. Aravindan, S.B. Lee, I.C. Jang, H.H. Lim, G.J. Park, M. Yoshio, Y.S. Lee, J. Alloys Comp. 504 (2010) 224–227.
[15] V. Aravindan, S. Ravi, W.S. Kim, S.Y. Lee, Y.S. Lee, J. Colloid Interface Sci. 355 (2011) 472–477.
[16] V. Aravindan, K. Karthikeyan, K.S. Kang, W.S. Yoon, W.S. Kim, Y.S. Lee, J. Mater. Chem. 21 (2011) 2470–2475.
[17] V. Aravindan, K. Karthikeyan, S. Amaresh, Y.S. Lee, Electrochem. Solid-State Lett. 14 (2011) A33–A35.
[18] V. Aravindan, K. Karthikeyan, S. Ravi, S. Amaresh, W.S. Kim, Y.S. Lee, J. Mater. Chem. 20 (2010) 7340–7343.
[19] V. Aravindan, K. Karthikeyan, J.W. Lee, S. Madhavi, Y.S. Lee, J. Phys. D Appl. Phys. 44 (2011).
[20] K. Karthikeyan, S. Amaresh, V. Aravindan, H. Kim, K.S. Kang, Y.S. Lee, J. Mater. Chem. A 1 (2013) 707–714.
[21] K. Karthikeyan, S. Amaresh, V. Aravindan, W.S. Kim, K.W. Nam, X.Q. Yang, Y.S. Lee, J. Power Sources 232 (2013) 240–245.
[22] C.G. Son, H.M. Yang, G.W. Lee, A.R. Cho, V. Aravindan, H.S. Kim, W.S. Kim, Y.S. Lee, J. Alloys Comp. 509 (2011) 1279–1284.
[23] M.S. Whittingham, Chem. Rev. 104 (2004) 4271–4302.
[24] C. Mason, A. Kannan, ISRN Nanotechnol. 2011 (2011) 708045.